 DOI: 10.20858/tp.2025.20.4.15

Keywords: two-mass system; nonlinear systems; mathematical simulations; frequency response

Merab CHELIDZE[1]*, Victor ZVIADAURI[2], Tamaz NATRIASHVILI[3], Alexandre DIDEBULIDZE[4], Gela JAVAKHISHVILI[5], Teimuraz KUNTCHULIA[6]

VIBRATIONAL TRANSPORT OF MATERIALS CONSIDERING THE PHYSICAL AND MECHANICAL CHARACTERISTICS OF THE "MATERIAL-WORKING ELEMENT" SYSTEM

Summary. This report examines the effect of the mass of the transported material on the dynamics of vibration machines. It is demonstrated that the structure of the transported materials (bulk or homogeneous lump) has a significant impact on the stability of the vibration modes of vibration machines. Mathematical modeling has demonstrated that the elasticity of the transported materials significantly affects the dynamics of vibration displacements and can cause both an increase and a decrease in vibration displacements, potentially leading to the reverse process of material displacement, as confirmed by experimental studies. Mathematical modeling has shown that the frequency, magnitude of the vibration amplitude, angle of inclination of the working body, and nature of the transported material significantly affect the process of vibration transportation and the power consumption of the vibration machine.

1. INTRODUCTION

Vibratory transport is used to move bulk and lump materials, blanks and parts in horizontal, inclined and vertical directions over distances from 0.5 to 100 m (and sometimes more) at factories, plants, mills, construction sites, mines, quarries, etc., as well as for feeding spatially oriented blanks and parts into technological devices, including those located in automatic lines [1-4]. Vibration equipment is used in medicine as miniature dental drills, in various automatic lines for dosed and oriented feeding of materials, transportation, separation, compaction, pressing, crushing, screwing, loosening, as well as at mining enterprises and nuclear power plants as powerful vibration equipment, where human presence is undesirable. Most vibration equipment, including electromagnetic vibrators, is characterized by high reliability in operation and low maintenance capital costs due to the absence of rubbing surfaces. In addition, they are inexpensive to produce [1, 4].

Fig. 1 shows an electromagnetic vibration machine consisting of: 1 − active mass, 2 − reactive mass, 3 − working body (connected to the active mass), 4 − elastic system (connecting the active and

[1] R. Dvali Institute of Machine Mechanics; Mindeli 10, 0186 Tbilisi, Georgia; e-mail: M.Chelidze47@gmail.com; orcid.org/0000-0001-8246-7533
[2] R. Dvali Institute of Machine Mechanics; Mindeli 10, 0186 Tbilisi, Georgia; e-mail: v_zviadauri@yahoo.com; orcid.org/0000-0001-7299-5770
[3] R. Dvali Institute of Machine Mechanics; Mindeli 10, 0186 Tbilisi, Georgia; e-mail: t_natriashvili@yahoo.com; orcid.org/0000-0001-9141-3641
[4] Georgian National Academy of Sciences; 52, Rustaveli Ave. 0108, Tbilisi, Georgia; e-mail: adidebulidze@yahoo.com; orcid.org/0009-0007-0793-6476
[5] University of Georgia; Kostava 77a, 0171, Tbilisi, Georgia; e-mail: gela.javakhishvili@ug.edu.ge; orcid.org/0009-0005-3633-7523
[6] Georgian Technical University; Kostava 77, 0175, Tbilisi, Georgia; e-mail: t.kunchulia@gtu.ge; orcid.org/0009-0000-6745-2341
* Corresponding author. E-mail: M.Chelidze47@gmail.com

reactive masses), 5 − electromagnetic conductors (connected to both masses), and 6 − electric coils placed on magnetic circuits.

Although vibration equipment is a simple machine in design, the mathematical description of its working process is very complex and requires full application of the theory of oscillations and dynamics [1, 4-14].

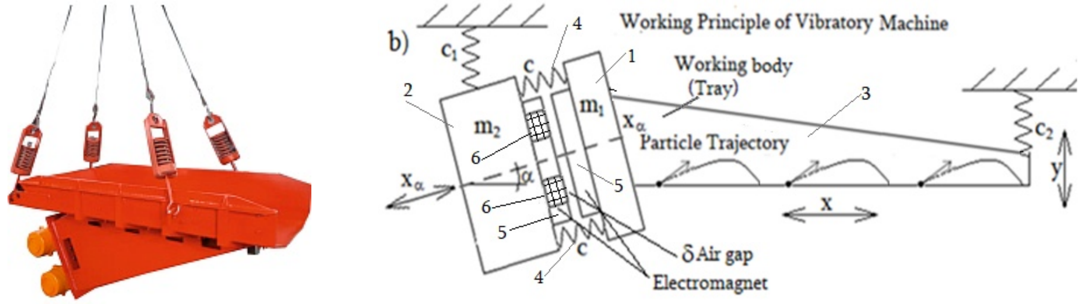

Fig. 1. a) Vibratory transport machine, b) diagram of vibration machine: 1 − active mass (m1), 2 − reactive mass (m2), c − elastic elements, c1, c2 − elasticity of suspension systems

The mathematical description of the technological loading process and its effect on the dynamic stability of a vibration machine's operating modes is an extremely challenging problem. Until recently, theoretical studies that account for technological loads in the dynamics of vibration machines have been largely absent, with only a few notable exceptions in recent literature [15-18]. Much work remains to be done, particularly considering the cyclic and nonlinear nature of technological loads, which can be critical for the stability of oscillation modes and the effective implementation of technological processes [19, 20].

We have addressed several key challenges in developing mathematical models of electro-vibration machines, particularly those related to nonlinear elastic-friction and electromagnetic excitation systems. These results have been presented at various international conferences and published in multiple scientific journals [21–24]. The working element of a vibration machine designed for tasks such as metered feeding, mixing, separation, and transportation of components performs elliptical motion. In other words, it simultaneously executes both vertical and horizontal oscillations.

It is also important to note that some scientific works present overly complex physical and mathematical models of vibration resistance and material processing in vibration systems, making practical calculations difficult [3, 8, 11]. The present work excludes secondary factors by adopting a simplified physical model. A mathematical model and corresponding simulator are developed based on engineering approximations and publicly available differential equations.

2. INFLUENCE OF PHASE SHIFTS BETWEEN DISPLACEMENT, VELOCITY, AND ACCELERATION OF TRAY OSCILLATIONS ON THE MOVEMENT OF TRANSPORTED MATERIAL

In the mathematical modeling of material vibration displacement, it is essential to account for the mutual 90° phase shifts between vibration displacement, velocity, and acceleration of the working body. These phase shifts play a critical role in the dynamics of vibration machines and in the process of material displacement under vibrational influence.

The alternating force generated by the vibrational acceleration of the machine's working body is shifted by 180° relative to the vibrational displacement. This force, together with the gravitational acceleration g of the m_t material, creates a periodic cyclic increase and decrease of the m_t pressure on the working body of the vibration machine.

Experimental and theoretical studies have demonstrated that vibrational displacement strongly depends on the amplitude, velocity, and acceleration of the vibrating body (tray), as well as on the frequency of its phase-contact interactions with the material m_t. Therefore, it is important to examine this phenomenon in detail.

Fig. 2a presents the amplitudes of vibration displacement, velocity, and acceleration of the working element obtained through mathematical modeling, considering the corresponding phase shifts. Fig. 2b shows the same parameters obtained experimentally.

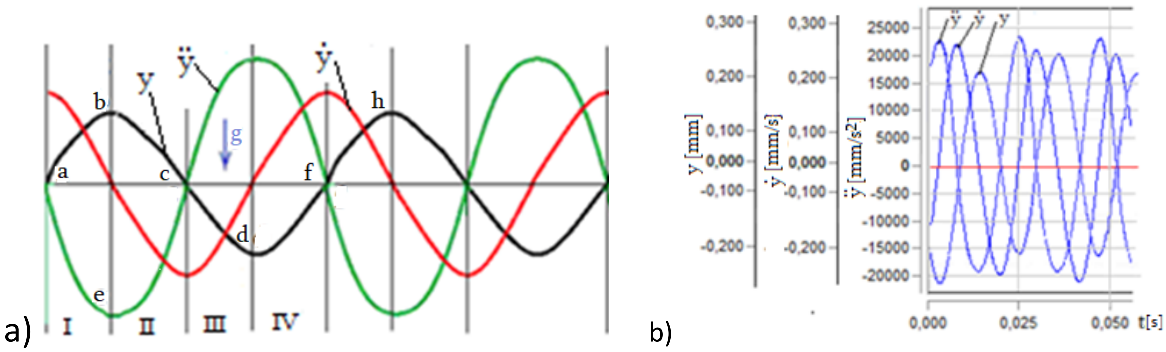

Fig. 2. a) The vibration displacement (y), velocity (ẏ), and acceleration (ÿ) were determined analytically. b) These parameters were also measured experimentally. In both analytical and experimental results, the parameters exhibit a 90° phase shift relative to one another

When the direction of the force caused by the vibration acceleration aligns with the direction of gravity (Periods I and II), the gravity force is subtracted from the vibration acceleration force. Conversely, in Periods III and IV, the vibration acceleration force adds to the gravity force. In other words, during Periods I and II, when $\ddot{y}$-g>0, the process mass dethatches from the tray, and when $\ddot{y}$-g<0, the pressure of the materials on the tray decreases. In Periods III and IV, the pressure of materials on the tray increases.

At the beginning of the first period, when the oscillatory motion of the tray y is minimal (i.e., $y = 0$) and the oscillation velocity $\dot{y}$ is at its maximum, while $\ddot{y}<g$, the pressure of the material on the section *ab* decreases, and the material begins to slide along the tray. As the amplitude of the tray displacement y increases and the velocity of the tray $\dot{y}$ decreases, the pressure of the material continues to reduce, facilitating further sliding along the tray.

At low vibration amplitudes or frequencies (i.e., when $\ddot{y}<g$), the process mass m_t remains in contact with the tray. However, when the vibration acceleration exceeds gravitational acceleration $\ddot{y}>g$, a micro-throw of material m_t occurs with an initial maximum vibration velocity $\dot{y}_0$. During the first period, the amplitude of the vibration displacements y increases, though its rate of increase in section (ab) diminishes. At the same time, the rate of increase of vibration acceleration $\ddot{y}$ (section ae), which acts in antiphase (180° shift), decreases. In the second period, both vibration displacement (section bc) and vibration acceleration (section ce) decrease, but the rate of the acceleration decrease is higher. It should be noted that, at small amplitudes in section bc, under the condition $\ddot{y}>g$, the vibrating tray leads the process mass m_t, causing it to detach from the tray. This detachment ends when m_t is reattached to the tray in section (df) (see Fig. 6a).

If the initial velocity of m_t at point (a) is sufficiently high (Fig. 2a), reattachment may not occur immediately in sections (ab or fh). Instead, it occurs in later sections, such as a-b, or f-h, or d-f, where the vibration velocity $\dot{y}$ is low or approaches zero. Thus, the process mass m_t, after being thrown with a high velocity from point (a or f), returns to the section (ab or cdf). In summary, the process mass m_t consistently detaches from the vibrating tray when the displacement y is minimal (i.e., at point (a or f) at the end of section d-f).

3. DYNAMICS OF VERTICAL OSCILLATION OF MATERIALS

Numerous theoretical and experimental studies have shown that the material velocity m_t is significantly influenced by the vertical component of the vibration machine. Fig. 3 presents oscillograms of the vertical motion of a 1-kilogram steel part on a vibration machine operating at a frequency of 50 Hz. Notably, this experimental oscillogram, which records the vertical movement of the material, was obtained for the first time using a digital electronic vibrometer and represents a novel contribution To minimize the influence of the sensor's mass on the frequency, amplitude, and waveform of the material's oscillations, the sensor was chosen to have a mass significantly smaller than that of the material. At large tray oscillation amplitudes (i.e., during most of the trajectory above the zero line in Fig. 3), the steel part (1) moves along the tray with intermittent detachment from it (2). At smaller amplitudes (when the contact pressure decreases), the steel part slides along the tray without separating. In the part of the trajectory below the zero line, the steel part is pressed against the tray with increased force and moves with it, experiencing minor jolts during lateral turns.

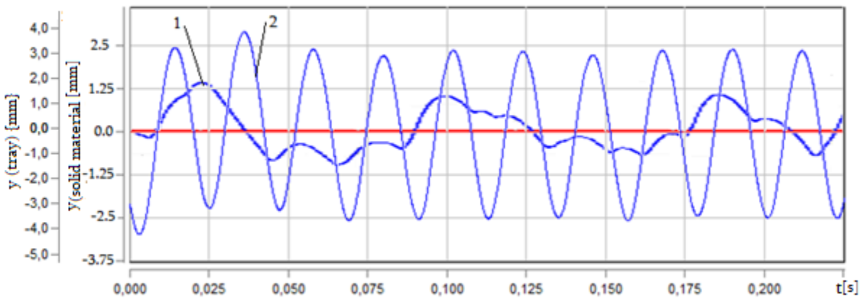

Fig. 3. Vertical vibro-oscillograms: 1 - Steel part; 2 - Working body (tray)

Fig. 4 illustrates the vertical oscillatory motion of the same 1-kg steel part placed on a rigid tray. The figure also includes an oscillogram where the steel part is placed on the tray through a soft, porous rubber base.

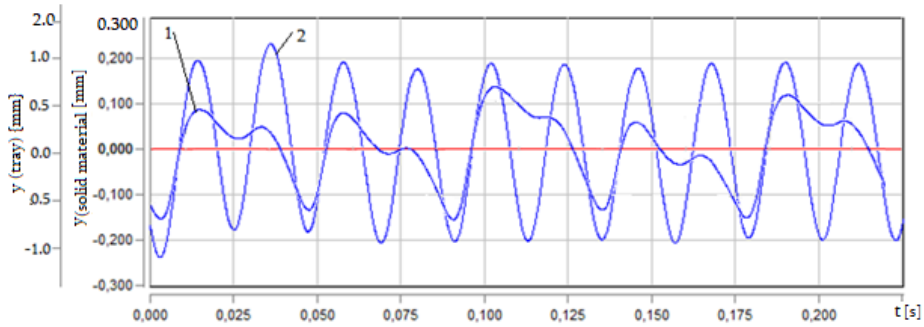

Fig. 4. Vertical oscillograms: steel part on a rigid surface and on a rubber cushion

These oscillograms (Figs. 3 and 4) demonstrate how the ratio of mass and elasticity affects the shape and frequency of the material's oscillations, regardless of the tray's own vibration characteristics.

The oscillatory motion of an electromagnetic vibrator is described by the following differential equations [6, 17, 20].

$$m\ddot{y} + n\dot{y} + cy = F(t) = k\Phi^2 \quad (1)$$

$$\dot{\Phi} + b\cos(\omega t) - c_0(\delta - y)\Phi; \quad , \quad (2)$$

where, m − Mass of the vibrator, c − Stiffness (spring constant) of the elastic elements, n − Damping coefficient (viscoelastic model), t − time, Φ- Magnetic flux, $k\Phi^2$ − Electromagnet excitation force, ω − Angular (circular) frequency of the exiter force, δ − Air gap between magnetic cores, b and c_0 − Proportionality coefficients; y, $\dot{y}, \ddot{y}$ − Displacement, velocity, and acceleration of vertical oscillation.

The vertical motion of the process mass, when separated from the active mass of the vibration machine [14], can be described by

$$y_m = \dot{y}_0 t - gt^2/2 \quad , \tag{3}$$

where y_m − Vertical displacement (trajectory) of the mass, y_0 − Initial velocity, g − Aacceleration due to gravity. Air resistance is not taken into account in Equation (2).

Fig. 5 is an oscillogram of vertical micro-throw movements of a lump part on a vibration machine vibrating at a frequency of 50 Hz, obtained using a simulator based on the differential equations (1)-(3). It should be noted that C++ Builder 6 was used for programming, mathematical modeling, and simulation.

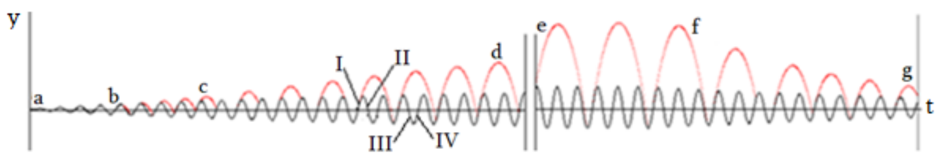

Fig. 5. Detaching and reattaching of material in the vertical direction, obtained by mathematical modeling at 50 Hz

The oscillogram shows that at low amplitudes, only pressure changes occur, (i.e., the material remains in contact with the tray (segment a–b)). As the oscillation amplitude increases, detachment and reattachment begin in each cycle (segment b–c, red), and with further amplitude increases, the separation-attachment cycle skips certain oscillation cycles of the tray (segments c–g, d–e).

According to the oscillogram, the process mass detaches from the vibrator at the maximum amplitudes of phase I of the oscillations and returns to the oscillating tray during phases IV or I of the oscillations.

Fig. 6 shows the same separation-attachment process at a lower frequency of 25 Hz.

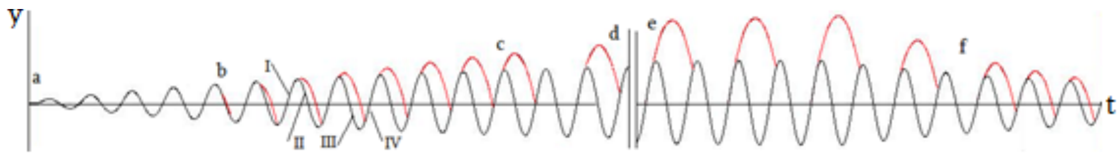

Fig. 6. Detachment and attachment dynamics at 25 Hz, based on mathematical modeling

According to the vibration oscillograms, at small amplitudes in section (a–b), the technological mass oscillates without detaching from the tray. In this range, only the pressure of the transported material varies, leading to corresponding changes in the friction force. As the vibration amplitude increases in section (b–c), the technological mass detaches from the vibrating plate during period I and reattaches during period III. At relatively high amplitudes (within sections (b–c) and (c–d)), the mass m_t detaches during the first period and reattaches in either the first or the fourth section. Notably, in these regions, the detachment and reattachment of the mass m_t occur by jumping across several adjacent amplitude levels. This jumping behavior becomes more pronounced at a vibration frequency of 50 Hz.

Furthermore, micro-throws of the process mass can be observed beginning near point (b). As the vibrating tray frequency (and thus the acceleration) increases, the amplitude values at which mass separation m_t begins decrease. As a result, a greater number of adjacent oscillating amplitudes are surpassed. Notably, the vertical velocity of m_t is largely unaffected by the magnitude of the friction force.

To illustrate the influence of the process load on vibration dynamics, we first consider only vertical oscillations. The attachment and detachment of a large mass from the tray can be modeled as a periodic impulsive force, in accordance with the law of conservation of momentum. Fig. 7 presents simulations of the oscillator's response to a single impulsive force of N=1000 N·s, applied at various oscillation phases.

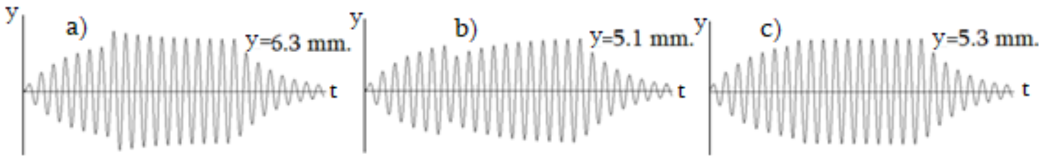

Fig. 7. Impulse force applied at different phases on a tray vibrating at a frequency of 50 Hz

In Fig. 7a, the amplitude of the oscillation increases due to the action of the impulsive force. In contrast, Fig. 7b shows a decrease in oscillation amplitude. Meanwhile, in Fig. 7c, the effect of the impulsive force is not observed. These oscillograms clearly demonstrate that the response of the oscillatory system is highly dependent on the phase at which the pulsed force is applied, a dependency that is particularly pronounced in the presence of lump (solid) material.

This phase sensitivity becomes more pronounced in an elastic system tuned to a 25 Hz resonant mode, where the system stiffness is reduced by a factor of four. The excitation power for oscillations at 25 Hz was reduced by a factor of 2.5 to maintain the same amplitude values as at 50 Hz (Fig. 8).

In the 25 Hz resonant mode, single actions of the pulse force N=1000 N·s cause completely different dynamic processes, in contrast to the 50 Hz mode [21-24].

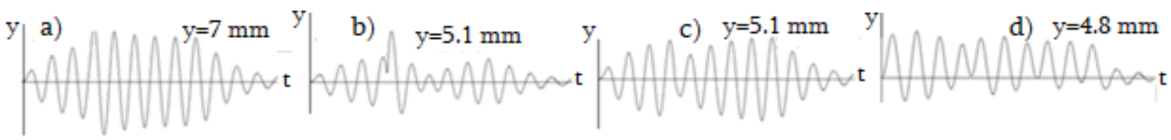

Fig. 8. Impulse response at 25 Hz resonant mode with reduced stiffness

Fig. 9 shows the jumping motion of a rigid body dropped from a height of 3 mm onto a static surface, showing different restitution coefficients (k=1, k=0.9, k=0.5). Fig. 10 shows the rebound delay due to elastic deformation at impact when the object drops on a soft rubber base with elasticity c_x.

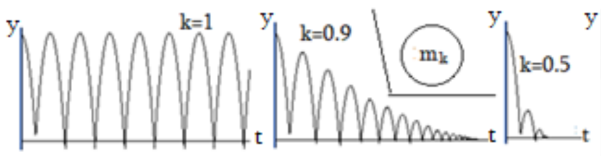

Fig. 9. Jumping of a rigid body at various restitution coefficients

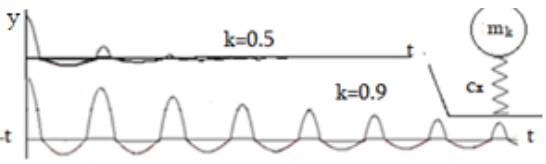

Fig. 10. Delayed rebound of an elastic body on a soft base

The oscillograms demonstrate that increased damping reduces both the frequency and amplitude of rebound of material. At a recovery coefficient of k=0.5, rebound virtually disappears. Therefore, for most materials subjected to vibrational displacement, subsequent multiple jumping events caused by material rebound can be neglected, as the recovery coefficient for most materials is typically below 0.3. Due to the cyclic changes in pressure on the tray during the detachment and reattachment of the material being moved, both the mass of the vibratory machine and its natural frequency vary. In some cases, this can lead to unstable resonant amplitudes.

This instability is particularly evident in resonant machines operating at 25 Hz when transporting large, dense, lump materials (Fig. 11a). However, with bulk (granular) material of the same mass, this resonant instability is significantly reduced or even absent (Fig. 11b) [22, 24].

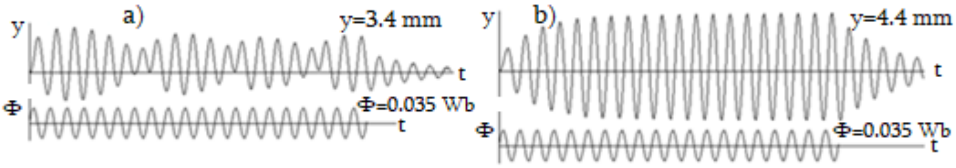

Fig. 11. a − Resonant instability with lump material; b – Stable resonance with bulk material

The above analysis highlights the importance of accounting for boundary conditions (based on Fig. 5), cyclic vibration displacement, velocity, and acceleration, as well as the physical and mechanical properties of the transported material and gravity, when creating a mathematical model or simulator for vibratory material transport.

4. VIBROTRANSPORTATION OF MATERIALS

In vibratory material transportation using a vibratory machine, the tray of the active mass (i.e., the working surface) is inclined at an angle of α=20° from the x_α-x_α direction of oscillation of the active and reactive masses (Fig. 1b). As a result, the working element performs an elliptical motion in space, performing both vertical $y=x_\alpha \cdot \sin\alpha$ and horizontal $x=x_\alpha \cdot \cos\alpha$ displacements. These are due to a variable exiting force inclined at 20°. To describe the motion of the transported material in the x–y plane, it is necessary to account for vibrational displacements in both the x and y directions, as well as the acting vertical (gravitational) and horizontal (exiting) forces.

At this stage, we consider a simplified system of differential equations describing the oscillations of an electromagnetic vibration machine, reduced to a single mass [24]:

$$(m+m_t)\ddot{y} + n\dot{y} + cy = 0.34k\Phi^2; \tag{4}$$

$$(m+m_t)\ddot{x} + n_0\dot{x} + cx = 0.94k\Phi^2; \tag{5}$$

$$\dot{\phi} + b\cos(\omega t) - c_0(\delta - x_\alpha)\Phi; \tag{6}$$

$$y = y_0 + \dot{y}_0 t - gt^2/2. \tag{7}$$

It should be noted that tilting the working element by 20° results in both vertical oscillations and partial rotational oscillations in the vertical plane (i.e., half-turning), which slightly alters the material's velocity along the tray [4, 8, 20]. When transporting material in the horizontal direction, the sliding movement of the transported mass m_t increases the dissipation coefficient n_0, as the sliding (useful work) introduces additional dissipative forces proportional to $n_0\dot{x}$.

To transform differential equations (4) and (5) into a form suitable for numerical solution using the Runge–Kutta method, it is necessary to divide these equations by the mass m of the vibrator, taking into account the attachment and detachment periods of the technological mass m_t.

$$\ddot{y} + 2h\dot{y} + \omega^2 y = 0.34P\Phi^2; \tag{8}$$

$$\ddot{x} + 2h_0\dot{x} + \omega^2 x = 0.94P\Phi^2, \tag{9}$$

When the mass m_t is attached, the natural frequency of the machine is given by $\omega^2 = c/(m+m_t)$ and the power factor is $P = k/(m+m_t)$. When the mass m_t is detached, the corresponding expressions become $\omega^2 = c/m$ and $P = k/m$. It should be noted that the attachion and detachion of the m_t to the working body also significantly affect the value of the damping coefficient $2h$ and $2h_0$. It should be noted that attaching or detaching the mass m_t from the working body also has a significant effect on the values of the damping coefficients $2h$ and $2h_0$.

Thus, the process of attaching and detaching the technological mass leads to a certain change in the mass and the resonant frequency of the vibrating machine, as described in the following works [6, 17–20].

Studies show that the cyclic variation of m_t leads to periodic changes of the reductive mass of the vibration system, imparting a soft nonlinearity to the system. A similar resonance shift is observed in the system shown in Fig. 12 (obtained by direct frequency calculation), where two springs of different stiffness are applied to a mass *m* without rigid fixation [25]. The amplitude–frequency response (AFR) obtained by mathematical modeling for this system (depicted in Fig. 13) shows resonance at 34 Hz with the following system parameters: m=1 kg, c_1=98596 N/m (50 Hz), and c_2=24548 N/m (25 Hz). Mathematical modeling also reveals a superharmonic resonance at 66 Hz.

Since ω^2=c/m, both stiffness c and mass m influence the resonance characteristics in opposite ways. Increasing c increases the resonant frequency, while increasing m decreases it. Both theoretical and experimental findings have validated this.

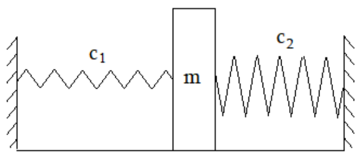

Fig. 12. An oscillating mass with loose elastic elements on the sides

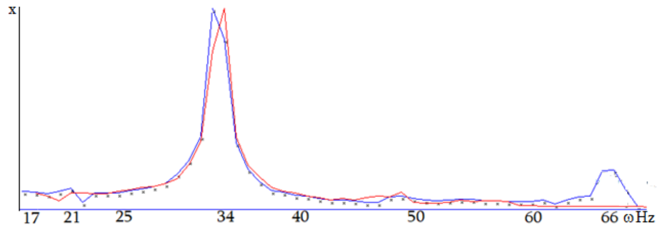

Fig. 13. AFR of cyclically changing stiffness

Fig. 14 shows the frequency response of a lump material undergoing periodic attachment and detachment. This response is similar to the one shown in Fig. 13. Fig. 15 presents the frequency response for a loose material. In this case, since the separation and reattachment of bulk material occur gradually (i.e., depending on the vibration amplitude, unlike lump materials, which separate instantaneously), a weakly nonlinear frequency response is observed.

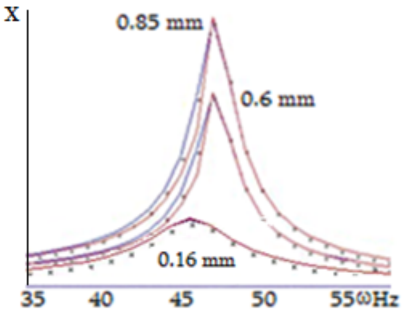

Fig. 14. AFR of cyclically detached/attached lump material

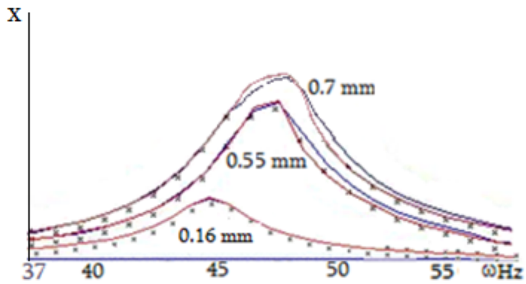

Fig. 15. AFR of cyclically and gradually detached/attached loose material

According to the oscillograms, adding 0.25 kg of process mass to a 1-kg machine with vibration amplitudes x<0.05 mm causes a resonant peak at 44 Hz, which gradually increases to 47 Hz with increasing amplitude. For lump material (Fig. 14), the resonance shifts almost abruptly from 45 Hz to 47 Hz. For bulk material (Fig. 15), the shift occurs gradually due to partial, gradual separation. To effectively utilize resonance, vibratory machines are designed with an unloaded resonant frequency of approximately 53–55 Hz, which ensures a resonant frequency of 50 Hz under operating conditions, corresponding to the industry standard of 50 Hz.

It is worth emphasizing that these AFRs under the influence of a cyclically changing mass were obtained through mathematical modeling for the first time; previously, such resonance shifts were determined only experimentally. Practically, the shift is approximated by adding 1/3 of the mass m_t to the total system mass [4, 6].

The moving mass m_t, located on the working element of the vibration machine, is subjected to a friction force $F_t=f_k m_t g/s$, where s is the contact area. In addition to the vertical force $F_y=m_t\ddot{y}$, the mass also experiences a horizontal force $F_x=m_t\ddot{x}$. The alternating vertical acceleration $\pm\ddot{y}$ changes the pressure of the moving mass of material on the tray in accordance with the phases of the vibration cycle.

While the acceleration $\ddot{x}$ remains less than the frictional acceleration $f_k(g \pm \ddot{y}/s)$, the condition $\ddot{x} < f_k(g + \ddot{y}/s)$ is satisfied. In this case, the mass m_t oscillates without slipping, moving together with the vibrating tray. Once the condition $\ddot{x} > f_k(g - \ddot{y}/s)$ is met, the sliding of the material m_t on the tray begins. At this point, the coefficient of static friction f_k is transformed into the coefficient of sliding friction f_s.

Fig. 16 shows 1 – the vertical vibration displacement of the material m_t; 2 – the vertical oscillation of the working body of the vibratory machine; 3 – the vertical vibration velocity of the material m_t; 4 – the horizontal vibration velocity of the material m_t, shown at a reduced scale.

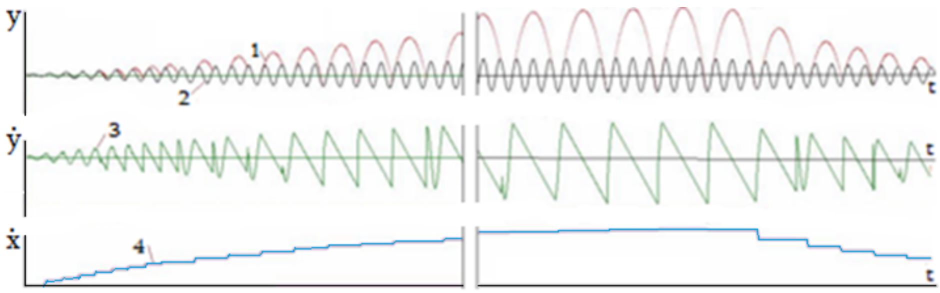

Fig. 16. Vertical and horizontal vibration velocities of m_t material

According to oscillograms 3 (vertical) and 4 (horizontal), the process of increasing and decreasing pressure of the mass of material moving along the tray of the vibration machine (along with the coefficient of friction and the detaching-attaching phases) has a significant influence on the speed of the material's vibratory movement [24].

Figs. 17a and 17b illustrate 1 – the vertical movement of the material m_t; 2 – the movement of the vibrating machine's tray; 3 and 4 – the horizontal vibratory motion of the material m_t. The scale of vibratory movement of m_t 4 in Fig. 17b is reduced compared to that of 3 in Fig. 17a.

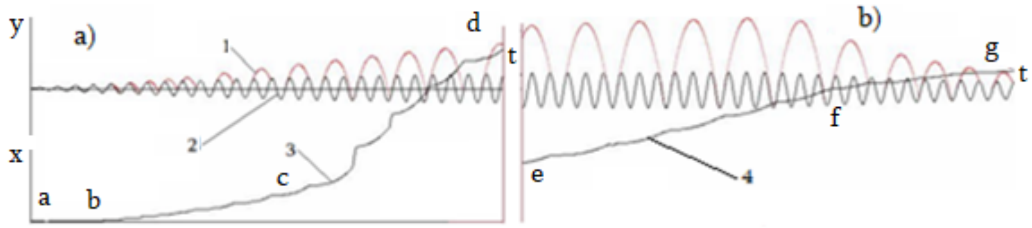

Fig. 17. Trajectory of horizontal movement of m_t material

An oscillogram of horizontal material vibration displacement, obtained using mathematical modeling, clearly demonstrates the influence of the vibrating machine tray vibrations and vertical micro-throws of the material m_t on the speed and shape of the displacement.

Fig. 18 shows 1 − the trajectories of vertical (red) and 3 − horizontal movements of the material, which are caused by 2 − the oscillation amplitude of the tray, vibrating at a frequency of 50 Hz. The horizontal movement trajectory of the material m_t along the working surface comprises a combination of sliding and flying phases, occurring sequentially during each vibration cycle. During the period τ_1, the pressure of the mass m_t on the surface of the working body decreases, because of which the movement of m_t along the tray occurs by sliding. During the period τ_1, the pressure of the material m_t on the surface of the working body decreases, resulting in sliding movement along the tray. During τ_2, the pressure increases, and the material moves at the horizontal speed of the working element $\dot{x}$, with minor slippage. During τ_3, the material undergoes a flight phase. During τ_4, the material moves opposite to the tray's motion. During τ_5, the flight phase concludes not at the peak of the adjacent oscillation cycle, but at that of the next cycle. During τ_6, the pressure between the material and the vibrator increases, and the movement occurs almost entirely at the horizontal speed of the vibrator.

Fig. 19 shows the reverse displacement mt, obtained through mathematical modeling. Region ab corresponds to forward motion m_t, region bc corresponds to sliding in place (without displacement), and region cd corresponds to backward motion. Mathematical modeling also showed that the additional soft elasticity of the m_t material at certain resonant amplitudes and frequencies leads to its reverse motion, which is confirmed by experiments. The reverse motion of the transported material is caused by changes in the phases of detaching and attaching the m_t to the vibrator, taking into account the elasticity of the attachment/detachment contact. Experimental and theoretical studies confirm that the speed of material desplacement m_t is significantly influenced by the frequency and amplitude of tray oscillations [6, 18, 20].

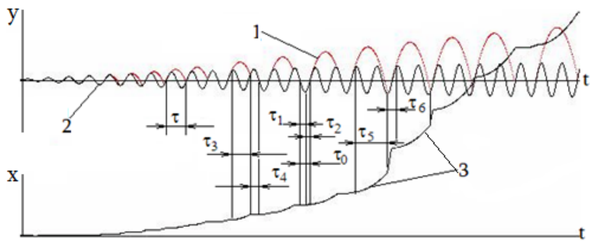

Fig. 18. Trajectory of vibration displacement of transported materials

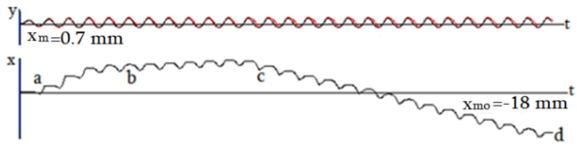

Fig. 19. Reverse displacement of m_t on an oscillating tray with a frequency of 50 Hz

The results obtained through mathematical modeling are in good agreement with experimental data (the error ranges from 5-10%). Horizontal vibratory displacement depends on the inclination angle α; specifically, greater vibration amplitudes require a smaller angle of inclination. The amplitude of vibratory displacement along the tray (x) primarily depends on the oscillation amplitude of the working element and averages around 90% of the horizontal component of that amplitude. Additional factors that significantly influence the magnitude of vibratory displacement include the coefficient of friction, cyclic material compression, and the phase of detachment–attachment, all of which are considered with respect to oscillation frequency.

It is essential to consider air resistance when mathematically modeling very light, dry, granular, and free-flowing powder materials. When exposed to vibration, light granules tend to float and disperse in the air, a phenomenon confirmed by experimental observations. In contrast, wet but light, free-flowing powders adhere to the tray and remain stationary relative to it. Vibratory displacement of such light, dry powders can only be effective under vacuum conditions.

5. CONCLUSIONS

A simplified physical model of a vibrational machine was used as the basis for developing a mathematical model and simulator described by differential equations commonly applied in engineering calculations.

Based on experimental and theoretical studies, a mathematical model describing the vibrational motion of materials was developed, and a corresponding mathematical simulator was created. Numerous computational experiments were conducted using this simulator. The results indicate that the elasticity of both the transported material and the working element (tray) has a significant impact on the stability of the vibration machines and the vibrational movement of the materials.

The results show that the elasticity of both the material to be moved and the working element (tray) significantly affects the stability of vibrating machines and the vibratory movement of materials. Given the complexity of vibrational displacement, mathematical modeling was performed in the vertical direction to clearly represent the influence of individual impulse forces (particularly those acting vertically) on the dynamics of the vibration machine, accounting for elastic-viscous effects.

Simulations further revealed that applying elastic or impulse forces generated at the moment the process load to the vibrator mass significantly impacts both the stability of the dynamic operating modes of the vibrator and the speed of material transport.

A comprehensive analysis of the phase shift parameters of vibration displacement, velocity, and acceleration of the working element is conducted. These parameters are essential for an accurate mathematical description of the material displacement process.

For the first time, the combined influence of the material detachment and attachment phases, along with the chute's oscillation phases, on machine dynamics and the material movement process was analyzed. The analysis considered oscillation frequency, contact elasticity, and amplitude. The study established that these parameters (and their ratios) play a significant role in determining the speed of material movement.

The study also reveals that the elasticity of the material and the working element, along with the coefficient of friction and the amplitude and frequency of oscillation, significantly influence the speed of material movement, which occurs through sliding and micro-throwing.

The results obtained from the simulator were compared with both the experimental results from this study and previous experiments (including those found in the scientific literature). This comparison confirms that the simulation results are in full agreement with experimental studies.

The obtained results were compared with the results obtained from experimental studies conducted in the course of the current work, as well as with the results of experiments we conducted in the early period and known from the scientific literature, on the basis of which it can be said that the results obtained with the help of the simulator fully correspond to the results obtained as a result of experimental studies.

Acknowledgments

This work was supported by Shota Rustaveli National Science Foundation of Georgia (SRNSFG) [FR – 24 – 1448, "Comprehensive research of the vibratory transport- technological processes and development of the designs of new, highly efficient devises"]

References

1. Блехман, И.И. *Вибрационная механика и вибрационная реология. Теория и приложения.* ФИЗМАТЛИТ. Москва. 2018. 752 p. ISBN 978-5-9221-1750. [In Russian: Blekhman, I.I. *Vibrational Mechanics and Vibrational Rheology. Theory and Applications*. Moscow. FIZMATLIT].
2. Han, L. & Gao, J.X. A study on the modelling and simulation of part motion in vibratory feeding. *Applied Mechanics and Materials.* 2010. Vol. 34-35. P. 2006-2010. DOI: 10.4028/www.scientific.net/AMM.34-35.2006
3. Fragassa, C. & Pavlovic, A. & Berardi, L. & Vitali, G. Investigation the dynamic behaviour of a linear vibratory feeder. *Proceedings on Engineering Sciences.* 2023. Vol. 05. No. 4. P. 709-720. DOI: 10.24874/PES05.04.013.
4. Вибрации в технике. Справочник в 6 томах. *Moscow Машиностроение.* 1978. T. 4. Vol. 4. 445 p. [In Russian. Vibrations in Engineering. *Handbook in 6 volumes. Mashinostroenie*].
5. Demidov, I.V. & Vaisberg, L.A. & Ivanov, K. Mechanics of granular materials under vibration action: Methods of description and mathematical modeling. *Enrichment of Ores.* 2015. Vol. 4. P. 21-31. DOI: 10.17580/or.2015.04.05.
6. Klemiato, M. & Czubak, P. Control of the transport direction and velovity of two-way reversible vibratory conveyor. *Archive of Applied Mechanics.* 2019. Vol. 89. P. 1359-1373. DOI: 10.1007/s00419-018-01507-8.

7. Burdzik, R. *Identification of sourses, propagation and structure of vibrations affecting man in means of transport based on the example of automotive vehicles*. Vol. 1. JVE International Ltd. April 2014. 245 p. ISBN: 978-609-95549-2-1. DOI: 10.21595/9786099603629.
8. Blekhman, I.I. & Vasilkov, V.B. & Semenov, Yu.A. On vibrotransportation of a material on a surface performing rotary oscillations. *Mekhanobr-Tekhnika REC, St. Petersburg, Russia.* 25 June 2019. P. 1-19. DOI: 10.21595/vp.2019.20745.
9. Kipriyanov, F. & Savinykh, P. The results of the study of the vibratory conveying machine operating modes. *Transportation Research Procedia.* 2022. Vol. 63(13). P. 721-729. DOI: 10.1016/j. trpro.2022.06.067.
10. Gzubak, P. Vibratory conveyor of the controlled transport velocity with the possibility of the reversal operations. *Journal of Vibroengineering*. 2016. 18(6). P. 3539-3547. DOI: 10.21595/jve.2016.17257.
11. Fragassa, C. & Pavlovic, A. & Berardi, L. & Vitali, G. Investigation the dynamic behaviour of a linear vibratory feeder. *Proceedings on Engineering Sciences*. 2023. Vol. 05. No. 4. P. 709-720. DOI: 10.24874/PES05.04.013.
12. Winkler, G. Analysing the vibrating conveyor. *International Journal of Mechanical Sciences***.** 1978. Vol. 20. No. 9. P. 561-570.
13. Schiller, S. & Steiner, W. & Schagerl, M. Extension of the bouncing ball model to a vibratory conveying system. *Nonlinear Dynamics.* 2023. P. 19685-19702. DOI: 10.1007/s11071-023-08911-y.
14. Chandravanshi, M.L. & Mukhopadhyay, A.K. Dynamic analysis of vibratory feeder and their effect on feed particle speed on conveying surface. *Measurement.* 2017. Vol. 101. P. 145-156. DOI: 10.1016/j.measurement.2017.01.031.
15. Despotovic, Z. & Stojiljkovic, Z. Power converter control circuits for two-mass vibratory conveying system with electromagnetic drive: simulations and experimental results. *IEEE Trans. Ind. Electron.* 2007. Vol. 54(1). P. 453-466. DOI: 10.1109/TIE.2006.888798.
16. Despotović, Z.V. A. & Ribic, A. & Šinik, V.M. Power current control of a resonant vibratory conveyor having electromagnetic drive. *Journal of Power Electronics*. 2012. Vol. 12. No. 4. P. 677-688. DOI: 10.6113/JPE.2012.12.4.6.
17. Despotović, Z. & Šinik, V. & Janković, S. et al. Some specific of vibratory conveyor drives. *V International Conference Industrial Engineering and Environmental Protection 2015* (IIZS 2015), October 15-16th 2015, Zrenjanin, Serbia. P. 247-254.
18. Despotovic, Z.V. & Urukalo, D. & Lecic, M.R. & Cosic, A. Mathematical modeling of resonant linear vibratory conveyor with electromagnetic excitation: simulations and experimental results. *Applied Mathematical Modelling*. 2016. Vol. 41. P. 1-24. DOI: 10.1016/j.apm.2016.09.010.
19. Elisseev, S.V. & Eliseev, A.V. *Theory of Oscillations: Structural Mathematical Modeling in Problems of Dynamics of Technical Objects.* Springer Cham. 2020. 152 p. ISBN: 978-3-030-31294-7. DOI: 10.1007/978-3-030-31295-4
20. Panovko, Ya.G. *Elements of the Applied Theory of Elastic Vibration*. Moscow. Mashinostroenie. 2020. 317 p. Available at: https://archive.org/details/panovko-elements-of-the-applied-theory-of-elastic-vibration/page/n3/mode/2up.
21. Chelidze, M. & Zviadaury, V. & Natriashvili, T. Some problems with the mathematical modeling of electromagnetic vibrators used for transporting bulk materials. *Transport Problems*. 2022. Vol. 17. No. 4. P. 55-66. DOI: 10.20858/tp.2022.17.4.05.
22. Zviadauri, V. & Chelidze, M. & Tedoshvili, M. *Dynamics of Vibratory Technological and Processes of Movement of the Friable Materials on the Spatially Vibratorin Plane*. LAMBERT Academic Publishing. 2021. 147 p.
23. Zviadauri, V. & Tumanishvili, G.G. & Tsotskhalashvili M. Mathematical model of complex control of the vibratory transportation and technological process. *Journal of Vibroengineering.* 2020. Vol. 22. No. 8. P. 1770-1781. DOI: 10.21595/jve.2020.20793.
24. Chelidze, M. & Tedoshvili, M. & Zviadauri, V. Dynamics of a rotating oscillating electromagnetic vibrator and unit grain displacement on an asymmetrically oscillating horizontal plane. *Problems of Mechanics*. 2022. Vol. 2(87). P. 33-41.

25. Светлицкий, В.А. & Стасенко, И.В. *Сборник задач по теории колебаний.* Москва. Издательство высшей школы. 1973. 205 p. [In Russian: Svetlitsky, V.A. & Stasenko I.V. *Collection of Problems in the Theory of Oscillations*. Moscow. Higher School Publishing House].

Received 10.03.2024; accepted in revised form 10.11.2025